HEFAT2014
10th International Conference on Heat Transfer, Fluid Mechanics and Thermodynamics
14 – 16 July 2014
Orlando, Florida

BENCHMARKING AND EVALUATING THE ACCURACY OF A LATTICE BOLTZMANN BGK SCHEME FOR MULTI-FLUID FLOWS

Yehya A.*, Naji H., and Zalewski L.
*Author for correspondence
Civil Engineering & Geo-Environment Laboratory (LGCgE-EA 4515),
Lille University, North France & Artois University/Faculty of Applied Sciences,
Technoparc Futura, F-62400 Béthune, France
*E-mail: alissar.yehya@gmail.com

ABSTRACT

Lately, the Lattice Boltzmann Method (LBM), as a mesoscopic numerical approach, has received more attention in studying complex fluid flows and transport phenomena. Because of its distinctive advantages over conventional numerical methods, the LBM has achieved great success in a variety of fields since its emergence. The major advantages are referred to its intrinsic linear scalability in parallel computing, and its capability of easily handling complex geometry and boundary conditions. In this study our proposed LB-BGK model, for multi-fluid flows, has been first validated by 2 benchmark problems: 2D Poiseuille flow problem and lid-driven cavity flow. Following these simulations, a discussion on the accuracy and the performance of the model is given. Good agreement is obtained with the analytical solution of Poiseuille flow problem, and with the available literature results for 2D lid-cavity. On the other hand, the accuracy of LBM is usually moderated by several factors; hence the effect of different factors is investigated. Among those, we studied the effect of boundary conditions, spatial resolution, Mach number, and that of the choice of relaxation factors. Consequently, LBM was found to be highly dependent on the physical problem, the numerical implementation, and the used models and correlations. In light of the obtained results, we can point out that the LBM may possess high potential in studying fluid flows with complex geometries.

INTRODUCTION

Lattice Boltzmann methods (LBMs) are mesoscopic particle based approaches to simulate fluid flows. Interest for LBMs has been growing continuously in the last 20 years [1], they are becoming a serious alternative to traditional methods for computational fluid dynamics (CFD) [2]. The method is historically originated from a Boolean fluid model known as the Lattice Gas Cellular Automata (LGCA), which simulates the motion of fluids by particles moving and colliding on a regular lattice [3]. Unlike traditional numerical methods, which solve for the macroscopic variables, the LBM is based on the kinetic equation for the particle distribution function. Hence, the macroscopic quantities are obtained through moment integration of the distribution function, and the averaged fluid variables are shown to satisfy the Navier-Stokes equations [3]. Due to the sampling of the particle velocities around zero velocity, LBM is limited to the low-Mach number (nearly incompressible) flow simulation. However some attempts have been made to extend the LBM to the compressible flow regime [4,5,6]. The interested reader can refer for example to [2,7,8,9] for details on this approach. Furthermore, LBMs are especially well suited to simulate flows around complex geometries [10], and flows in porous media; moreover they are straightforwardly implemented on parallel machines [11] due to their local nature.

NOMENCLATURE

f	[-]	Density distribution function
e	[lu/ts]	Lattice velocity
ω	[-]	Weight factor
τ	[-]	Relaxation parameter
ρ	[mu/lu^2]	Macroscopic density
u	[lu/ts]	Macroscopic velocity
v	[lu^2/ts]	Kinematic viscosity
Re	[-]	Reynolds number
Ma	[-]	Mach number

Subscripts

i	Velocity direction of lattice
w	Wall boundary
max	Maximum
0	Reference parameter

The availability of different LBMs made the choice of the type of model highly dependent on the competence of its accuracy over the computational speed. Among these types, we can cite the single relaxation-time lattice model, also called the Bhatnagar-Gross-Krook (BGK model), which is the most popular one for its simplicity. In order to effectively apply the

LB-BGK model; it seems crucial to achieve its limitations under variety of situations. Benchmarking a model under several well-known analytical solutions to physical problems is the best way to find and understand the accuracy and limitations of any computational scheme. In the first part, we propose and outline an LB-BGK model for multi-fluid flows. The model can simulate up to five fluids in a system. We then benchmark it, in the second part, via two different problems namely Poiseuille flow and 2D lid-cavity. In the last part, we intend to evaluate the accuracy of the model, is usually moderated by several factors. Of these, we examine the effect of boundary conditions, the spatial resolution, the Mach number, and that of the choice of relaxation factors.

BGK LATTICE BOLTZMANN MODEL

The starting point in the LBM relies on the transport Boltzmann equation, whose discrete form in the BGK approximation of the collision operator, reads as [12],

$$\frac{\partial f_i}{\partial t} + e_i.\nabla f_i = -\frac{1}{\tau_f}(f_i - f_i^{eq}) \quad (i = 1,2,\dots,N) \qquad (1)$$

where f_i is the particle velocity distribution function, e_i is the velocity along the *i*th direction, and *N* is the number of different velocities.

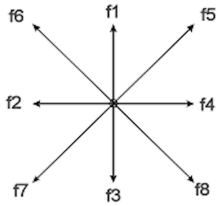

Figure 1. 2DQ9 lattice model

In the work, we employ the two-dimensional nine velocity (D2Q9) which is illustrated in Fig. 1. In Eq. (1), the f^{eq} is the local equilibrium distribution function, and it is defined as follows,

$$f^{eq} = \omega_i \rho[1 + \frac{3(e_i.\vec{u})}{c^2} + \frac{9(e_i.\vec{u})^2}{2c^4} - \frac{3u^2}{2c^2}] \qquad (3)$$

where $\omega_i = \begin{cases} 4/9 & for\ i = 0 \\ 1/9 & for\ i = 2,4,6,8 \\ 1/36 & for\ i = 1,3,5,7 \end{cases}$

and $e_i = \begin{cases} (0;0) & for\ i = 0 \\ (0;\pm 1) & for\ i = 2,4 \\ (\pm 1;0) & for\ i = 1,3 \\ (\pm 1;\pm 1) & for\ i = 5,6,7,8 \end{cases}$

are, respectively, the weight factor and the velocity vector of the D2Q9 model. The macroscopic quantities [12], such as density, ρ and momentum density, ρu, are defined as moments of the distribution function, f_i, as follows,

$$\rho = \sum_i f_i \text{ and } \rho u = \sum_i f_i e_i \qquad (4)$$

BOUNDARY CONDITIONS

To apply boundary conditions to a Lattice Boltzmann method, the distribution functions f_i at boundary lattice points have to be modified or replaced during each time step to give the required fluid velocity. There are different types of boundary conditions that can be easily handled in LBM, which constitutes a major advantage for this method. We state below some of these boundary conditions that will be used in this work.

On-grid bounce-back

The on-grid bounce-back condition applies a no-slip condition (i.e. zero fluid velocity) at a boundary that lies halfway between grid points. This is applied after the propagation process by reversing the distribution functions sitting on each wall node x_w, i.e.

$$f_i(x_w, t) = f_j(x_w, t) \qquad (5)$$

where *j* is the opposite lattice link to *i,* i.e. $e_j = -e_i$. The reflection of distribution functions occurs on-grid. Note that on-grid bounce-back is a first-order approximation of the boundary condition. Thus, the error is proportional to the lattice spacing Δx, while remaining completely local (i.e. only uses distribution functions at the wall node).

Mid-grid bounce-back

The mid-grid bounce-back condition also applies a no-slip condition at a boundary halfway between lattice points [2]. This is applied by assigning post-collisional distribution functions to the wall node based on those values at neighbouring points, i.e.

$$f_i(x_w, t^+) = f_j(x_w + e_i\Delta t, t^+) \qquad (6)$$

This method essentially applies the actual reflection halfway between time-steps and is a spatially second-order method, although it is weakly non-local due to its use of distribution functions from neighbouring nodes.

Constant pressure/velocity

To specify either velocities or densities (pressures) at planar boundaries, the Zou-He method [13] is used. This is based upon applying the bounce-back rule to the non-equilibrium distribution functions, i.e.

$$f_i^{(1)}(x_w, t) = f_j^{(1)}(x_w, t) \qquad (7)$$

where $f_i^{(1)} = f_i - f_i^{eq}$, with the equilibrium distribution function f_i^{eq} as a function of density and velocity. This function can be used to determine the missing wall velocity or density along with the known distribution function values. For instance, for a top edge with a known velocity $\overrightarrow{v_w}$ using the D2Q9 lattice scheme, the wall density and missing distribution functions (all for the boundary node at x_w) are given as:

$$\rho_w = \frac{f_0+f_2+f_6+2(f_1+f_7+f_8}{1+v_{w,y}} \quad (8)$$

$$f_4 = f_8 - \frac{2\rho_w v_{w,y}}{3} \quad (9)$$

$$f_3 = f_7 + \frac{1}{2}(f_6 - f_2) - \frac{1}{2}\rho_w v_{w,x} - \frac{1}{6}\rho_w v_{w,y} \quad (10)$$

$$f_5 = f_1 - \frac{1}{2}(f_6 - f_2) + \frac{1}{2}\rho_w v_{w,x} - \frac{1}{6}\rho_w v_{w,y} \quad (11)$$

BENCHMARKING THE LB-BGK MODEL

The current LB-BGK model was benchmarked using different physical problems and compared with the known analytical solutions [14] or the available numerical results of past works [15,16,17].

2D Lid driven cavity

The Lid driven cavity flow is one of the most common benchmark test problems.

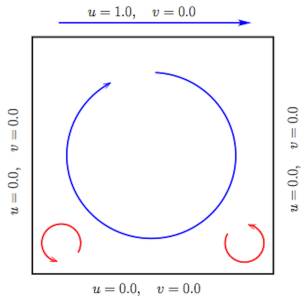

Figure 2. Geometry of lid driven cavity

The simplicity of the geometry of the cavity flow makes the problem easy to code and apply boundary conditions [18]. Briefly as shown in Fig. 2, a square cavity is filled with an incompressible fluid, which is governed by the Navier-Stokes equations where the flow is driven by the moving top wall. Furthermore, velocities at other boundaries are set to zero and non-slip boundary conditions are applied elsewhere. A characteristic of the 2D cavity flow is the emergence of primary vortex in the center of cavity, while with higher Re, secondary vortices appear in the lower corners. In our example, we choose a problem of *Re=100* and compare the results with available data in the literature. The profiles of the velocities in both x and y directions for the centreline, displayed in Fig. 3, resemble the available profiles from previous works. Moreover, the positions of the primary and secondary vortices are within acceptable conjunction with the available results as can be inferred from Table 1.

Pressure driven Poiseuille flow

The 2D pressure driven Poiseuille flow is another classical benchmark case. The pressure difference is accounted for by a density difference since they are proportional as per the equation of state. For our study, the following parameters, in lattice units, are adopted: the inlet and outlet pressures are 1.1mu/ts^2 and 1mu/ts^2 respectively, the channel width W is 50lu, the channel length L is 350lu, the relaxation factor τ_f is fixed at 1.5, the kinematic viscosity is ν=0.333lu^2/ts, and the reference density is taken equal to 3mu/lu^2.

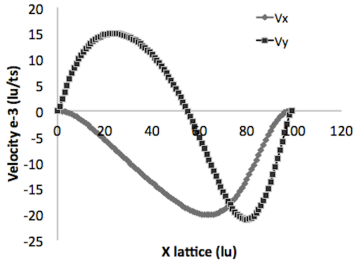

Figure 3. Velocity profiles at horizontal centreline of the cavity

Besides, for the left and right sides, constant pressure/velocity are used as boundary conditions while on-grid bounce back is used for the top and bottom sides. It is useful to recall that the analytical solution is,

$$U(y) = \frac{(p_{in}-p_{out})}{2\nu\rho_0 L}(Y - Y_{bottom})(Y_{top} - Y) \quad (12)$$

and

$$U_{max} = \frac{(p_{in}-p_{out})(Y_{bottom}-Y_{top})^2}{8\nu\rho_0 L} \quad (13)$$

Note that, in our model, $\Delta t = \frac{\nu}{c^2(\tau_f-0.5)}$ *and* $\Delta x = \frac{\sqrt{3}\nu}{c\,(\tau_f-0.5)}$

So by choosing $\nu = 1.5e^{-5}m^2/s$, $\Delta t = 5.144e^{-11}$ and $\Delta x = 4.81e^{-8}$. It should be noted that this induced value of ν has no physical effect. In other words, it just serves in the calculation of Δx and Δt and thus the physical width and time. In all cases the obtained results correspond to the steady state. Fig. 3 shows a comparison between the analytical and numerical solutions. The numerical results match the analytical solutions while the discrepancy is thought to be due to the choice of relaxation factor and boundary conditions. If the relaxation factor is changed to 5, the numerical results remain approximately the same as the analytical results (see Fig. 4). This issue will be thoroughly discussed later.

Re=100	**Primary Vortex**		**Lower Left Vortex**		**Lower Right Vortex**	
	x	y	x	y	x	y
A	0.6188	0.7357	0.0375	0.0313	0.9375	0.0563
B	0.6172	0.7344	0.0313	0.0391	0.9453	0.0625
C	0.6196	0.7373	0.0392	0.0353	0.9451	0.0627
D	**0.6161**	**0.7373**	**0.0404**	**0.0404**	**0.9370**	**0.0606**

Table 1. Locations of vortices of the lid-driven cavity flow at Re=100. A: Vanka [15], B: Ghia et al [16], C: Hou et al [17], D current work.

(a) (b)

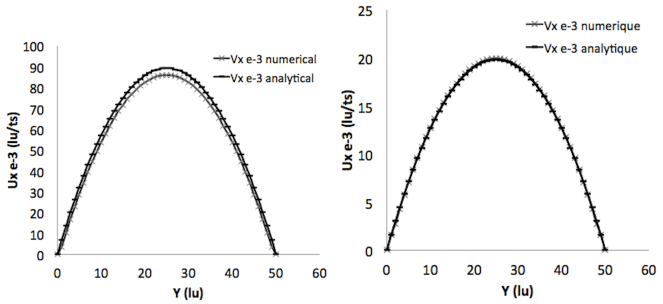

Figure 4. Comparison between analytical and numerical solutions for pressure driven Poiseuille flow $(a)\tau = 1.5, (b)\tau = 5$

Different simulations have been performed for different Reynolds numbers, where $Re = \frac{U_0 W}{\nu}$, U_0 being the reference velocity which is based on the imposed pressure gradient [19] as $U_0 = \frac{(p_{in} - p_{out})W^2}{2\rho\nu}$. As shown in Fig. 5, the maximum velocity increases with the increase in *Re*, and that is provoked by an increase in error when compared to the analytical solution. Such an error becomes significant after *Re=2083*, which points to the passage into a turbulent regime.

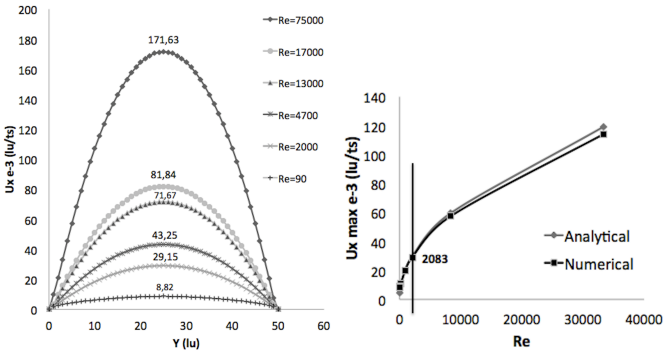

Figure 5. Comparison between numerical solutions of pressure driven Poiseuille flow for different Re

EVALUATING THE ACCURACY OF THE CURRENT LB-BGK MODEL

The increased use of the lattice Boltzmann method for the computation of fluid flow has generated the need for more rigorous documentation on the errors associated with the LBM. An important and significant source of error stems from the boundary conditions, the choice of relaxation factors, the geometry, the Mach number, and hence the Reynolds number that is affected by the mentioned parameters and by which different physical behaviours can be generated. In this section we study the accuracy for the above pressure driven Poiseuille flow problem with on-grid bounce back boundary conditions at top and bottom. We thus define the relative error to be [19],

$$err_i = \frac{|U_{i(numerical)} - U_{i(analytical)}|}{U_0} \qquad (14)$$

The relaxation parameter effect

It is known that the relaxation parameter defines the lattice viscosity. Hence, its choice affects the physical behaviour of the fluid, and it should be always > *0.57* to insure the stability of the model when using Zou/He boundary conditions. For the above problem we vary the relaxation factor τ from 1 to 20 while maintaining the same number of lattices (*W=50*), and investigate the impact on the accuracy of the model keeping in mind that we are also changing *Re* and *Ma*. In real parameters, the increase in τ will result in a decrease in both Δx and Δt, hence a change in space and time discretization. Accordingly in real physics this will mean a decrease in the width of flow and the reference velocity.

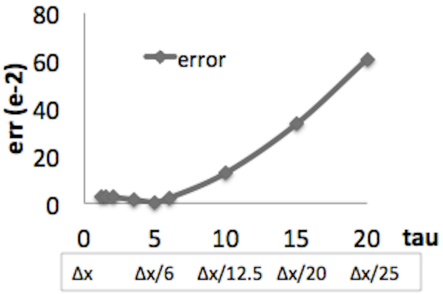

Figure 6. Error variation with the relaxation factor

The results show that increasing τ and hence decreasing Δx will moderately decrease the error (err_i) until a certain factor ($\tau = 5$) after which the error will start increasing rapidly (Fig. 6). In lattice parameters, this means increasing the lattice viscosity 5 times to reach the optimum accuracy for a lattice width of 50. Nevertheless, in real physics this corresponds to decreasing the space discretization 6 times to reach the optimum accuracy for a discretization of 50 lattices, after that the model discretization is too small and the accuracy is lost. This leads us to an important factor which is the discretization in space and time. As concluded from the above, there are limits for decreasing Δx and Δt to insure better accuracy for a given with *W*. It is observed that as *W* increases, the optimum value of τ decreases. Further studies will be performed in the next paragraph on the effect of *W* on the optimum discretization.

The lattice width effect

When keeping a constant relaxation factor, thus constant discretization parameters, the increase in W will result in a decrease in errors until a certain value of W after which the errors increase again. This can be explained, as the previous results, by the fact that the discretization should be neither too small nor too big for the domain. Increasing the domain insures that U_{max} is far enough form the boundary walls, which are the min source of errors, but afterwards the domain will become too big to preserve the needed accuracy. On the other hand, for each *W* simulated, we found the optimum τ, and realized that as *W* increased the optimum τ also increased linearly by a regression equation obtained with R-squared of 98.4%, and expressed as,

$$\tau_{optimum} = 0.0451W + 2.4855 \qquad (15)$$

Hence, for a given Reynolds number *Re,* the optimum $(\tau, W)_{opt}$ can be chosen satisfying (15) and (16)

$$Re = \frac{U_{ref}W}{\nu} = \frac{(p_{in}-p_{out})W^3}{2\rho\nu^2} = \frac{9(p_{in}-p_{out})W^3}{2\rho(\tau-0.5)^2} \qquad (16)$$

Consequently, for the pressure driven Poiseuille flow, we can, by using the above equations, optimize the accuracy by choosing the discretization domain. Similar optimization procedure can be undertaken for different benchmark problems with known numerical or analytical solutions.

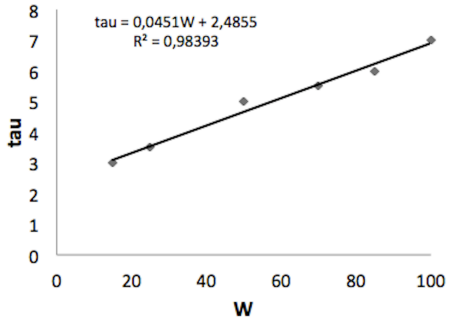

Figure 7. $\tau_{optimum}$ calculated for different values of W

Accuracy variation with Mach number

Recall that the LBM is a simplified version of the continuous Boltzmann equation as it is fully discrete in time and phase space. Due to the sampling of the particle velocities around zero velocity, LBM is limited to the low-Mach number (nearly incompressible) flow simulation. Nevertheless, recently many attempts have been made to extend the LBM to the compressible flow regime [4,5,6].

To study the effect of Ma on accuracy we performed a set of simulations for $\tau = 2, 3.5, 5, 6$ and we varied *Ma* for each between 0.02M, 0.05M, 0.07M, 0.1M, 0.2M, 0.3M, 0.4M, 0.5M, 0.6M, where M is a characteristic constant for each set, for example M=0.5144 for *τ=5* and then Ma ranges from 0.01 and 0.3. Generally, the accuracy increases as the Mach number decreases (such that it remains less than). This is clearly encountered when we varied the pressure difference for a given *($\tau = 5$, W=50)* and hence fixed *Re/Ma*. The errors undergo a parabolic increase with the increase of Ma as shown in Fig. 8a. However, it is noted that for lower relaxation factors, the effect of Ma is negligible, and for higher relaxation factors, for acceptable errors, the influence is less significant. Consequently, we regard this issue to the presence of low compressibility effect and hence low compressibility errors, which highly dependent on the *Ma* number. Moreover, for lower τ, the compressibility errors are too small in comparison with discretization errors and hence the effect of *Ma* is negligible. Besides for high τ, both compressibility and discretization errors are high, but the latter is the dominant. So the effect of Ma is found to be low in that case. Furthermore, we define the compressibility error to be [20],

$$\rho_{err} = (\Delta x)^2 \left[\left(\frac{\partial u_x}{\partial x}\right)^2 + \frac{\partial u_y}{\partial x}\frac{\partial u_x}{\partial y}\right] \qquad (17)$$

Clearly, the compressibility error depends on the grid spacing and the variation of velocity between neighboring lattices. Likewise, this analysis can provide information about the compressibility error independently from the discretization error. For *τ=5*, a change in error of u_x is noticed as *X* goes far from the vertical boundaries and an increase in error is noticed as *Y* approaches the centerline (Fig. 8a). This increase, hence, induces the increase in the velocity profile as it reaches its maximum in the centerline. Thus, for this case, the major source of error is the compressibility effect since the discretization error is too small and hence is highly affected by the variation in *Ma*, while for lower relaxation numbers the error is approximately constant with the variation of *Y* as indicated in Fig; 8b. However, the compressibility error remains small with respect to the discretization error and that is the reason why it is clear when choosing $(\tau, W)_{opt}$, and thus choosing a certain *Re/Ma*. On the other hand, for (τ, W) far from optimum, the major source of error is therefore the discretization in time and space whereas the compressibility error and the effect of Ma variation are negligible in comparison with it.

(a) (b)

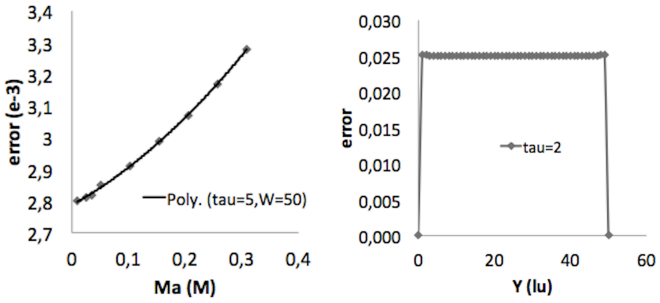

Figure 8. (a) Variation of error for *($\tau = 5$, W=50)* with the increase in *Ma*, (b) Variation of error along *Y* for *τ=2*

Summing it all up

Till this level, we have discussed the effect of each parameter alone. So as a summing up, we plotted errors in our simulations versus $S = \log\left(1000\frac{W.\tau}{Re.Ma}\right)$ to evaluate the global effect on the accuracy. As inferred from Fig. 9, when S<4.87 (an estimated inflection point), the errors are low and acceptable. Afterwards, the errors start increasing exponentially and thus will reach unacceptable results. Therefore as long as $\frac{W.\tau}{Re.Ma} < 74$, the errors are limited and acceptable. Otherwise, the errors will start increasing highly and the model looses its accuracy.

THE EFFECT OF BOUNDARY CONDITIONS ON THE ACCURACY

It is well known that the boundary conditions are the main source of errors in a model as unknown distribution functions

originated from the undefined nodes external to the flow domain are encountered during the streaming operation.

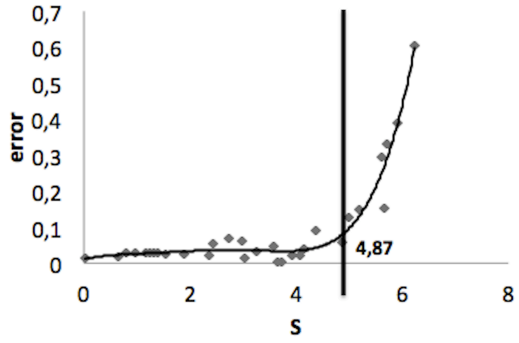

Figure 9. Variation of the error with the defined value S

In this section, the effect of changing boundary conditions is studied. The left and right boundary conditions in the pressure driven Poiseuille flow are always handled by fixed pressure/velocity boundary conditions. Our discussion will be mainly for the non-slip top and bottom sides where the velocity should be zero. We first simulate, for different relaxation factors, and thus discretization parameters, the model with on-grid bounce back boundary conditions. We then used the mid-grid boundary conditions described in the first section, and afterwards we simulated the model with fixed velocity with $v=0$ on top and bottom.

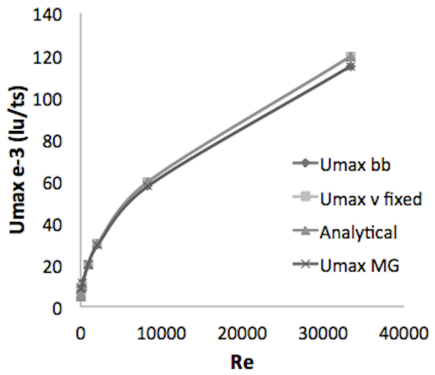

Figure 10. Comparison between U_{max} for different boundary conditions with the analytical solution

When comparing these three types of boundary conditions in the code, it is noted that there is very little difference in accuracy between the on-grid bounce back and the mid-grid bounce back. Nevertheless, if the bounce-back boundary condition is implemented on the boundary nodes, where the wall resides, the bounce-back boundary condition only gives first order accuracy, whereas if the bounce-back boundary condition is employed with the wall located at half-grid-spacing between a flow node and a bounce-back node, the scheme is shown to produce second-order accuracy. On the other hand, when using fixed velocity boundary conditions, the errors decrease and this is more significant for low relaxation factors. The maximum velocities for different Reynolds number are plotted for the three types of boundary conditions and compared to the analytical solution. The results of fixed velocity boundary conditions coincide with the analytical results as shown in Figure 10, while a small discrepancy is observed with the on-grid and mid-grid boundary conditions, which in return coincide with each other. Since the variation of errors is not substantial, we plotted the log of the errors versus the inverse of τ to better understand its variation.

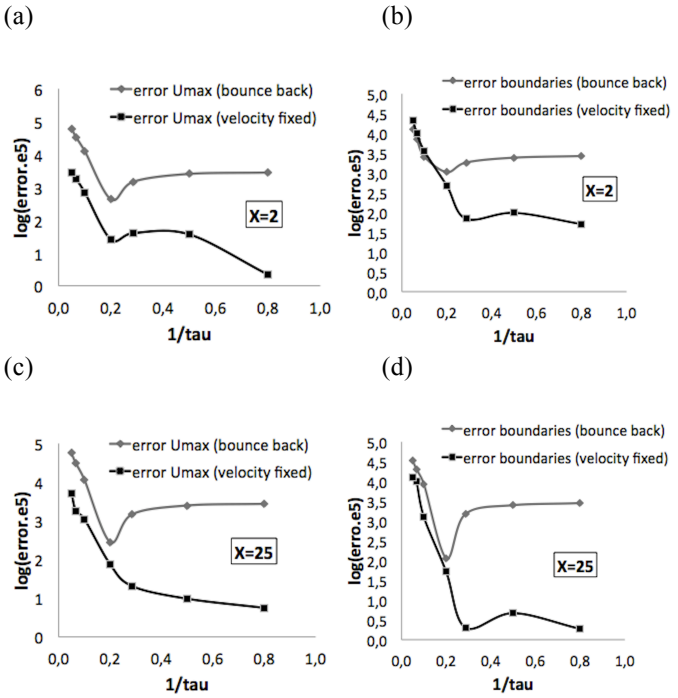

Figure 11 Comparison of the errors at centerline and boundaries for different boundary conditions and for selected positions of X

Fig. 11(a,c) shows a comparison between errors in bounce back and fixed velocity boundary conditions for U_{max}, while Fig. 11(b,d) indicates that for Y close to top and bottom boundaries. For high relaxation factors the difference is not important, whereas for low relaxation numbers the errors close to top and bottom are much less for fixed velocity, and evidently in this case the accuracy is better in lower τ and the optimum τ is close to 1. We also investigate the difference in the errors as we increase X from 2 to 25. We note a more relevant decrease in errors as we go further from the boundaries. Additional grids to extrapolate the distribution functions on boundaries can lead to more consistent boundary conditions and enhance the accuracy of the scheme. More details of this procedure can be found in [12]. Hence, another point that should be highlighted on is the effect of boundary conditions on compressibility errors, and we can recognize it clearly when comparing the errors along Y for different boundary conditions for the same X. As presented in Fig. 12, the difference in errors along Y is not significant for bounce back boundary conditions especially for low relaxation factors. While in contrary, errors decrease as we go far from top and bottom boundaries for fixed velocity boundary conditions, and are minimum at the center, for low relaxation factors. This

reveals the sensitivity of these boundary conditions to positions and relaxations factors. Thus despite of increase in accuracy it showed in comparison to bounce back, careful consideration should be taken to the non-homogeneity of the errors between adjacent nodes.

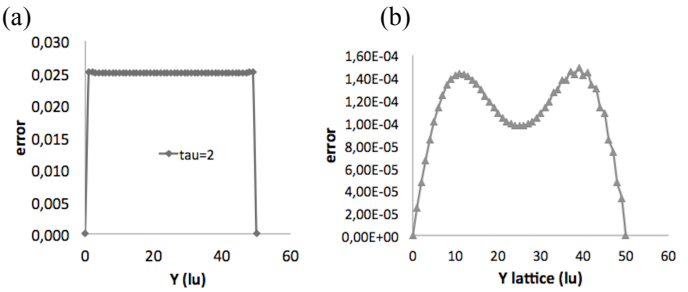

Figure 12. (a) error varaition along Y for bounce back boundary condition, (b) error varaition along Y for fixed velocity boundary condition

CONCLUSION

The proposed L-BGK model was benchmarked with two well-known benchmark problems. Good agreement is obtained with the analytical solution of Poiseuille flow problem, and with the available literature results for 2D lid-cavity. For the Poiseuille flow problem, the *Re* critical beyond which the regime becomes turbulent was found to be 2083, which matches the literature results [21]. Furthermore, the accuracy of the model was tested for different special dimensions and relaxation parameters. It was noted that these parameters have a clear influence on accuracy since they constitute the main source for discretization errors. On the other hand, for every studied width we have located its optimum relaxation factor, reaching an empirical expression to relate $(\tau, W)_{optimum}$. In addition, the effect Ma was studied, and as expected as Ma increases the accuracy decreases, however this is more significant when the discretization errors are very small i.e. when we use $(\tau, W)_{optimum}$. Unlikely, when the discretization errors are large enough, the compressibility errors are negligible and the effect of Ma is less significant. Moreover, a critical value of $W.\tau/Re.Ma=74$ was obtained, after which the model's errors increase heavily and it loses its accuracy. Finally, a comparison between different boundary conditions is established, and fixed velocity boundary condition showed more accuracy than the bounce back boundary conditions, especially for low relaxation factors, whereas the latter showed less compressibility errors and more uniformity of errors on adjacent lattices. As a conclusion, our results show that LBM is considerably competitive as a computational tool for fluid flow problems and if tuned by optimizing its accuracy and performance is capable of changing the landscape of CFD market.

ACKNOWLEDGEMENTS

The authors gratefully acknowledge the National Research Agency (ANR: French Agency) for its support in this study under the research project Stock-E "MICMCP".

REFERENCES

[1] Sukop M.C. and Thorne D.T., Lattice Boltzmann Modeling: An Introduction for Geoscientists and Engineers, *Springer*, 2006
[2] Succi S., The lattice Boltzmann Equation: for Fluid Dynamics and Beyond*, Series Numerical Mathematics and Scientific Computation, Oxford New York: Oxford University Press,* 2001
[3] Quan L., Tien-Chien J., Application of Lattice Boltzmann Method in Fluid Flow and Heat Transfer, *InTech*, ISBN 978-953-307-169-5, July 2011, pp. 29-32
[4] Mason R.J., A multi-speed compressible lattice Boltzmann model, *J. Statist. Phys., 107 (2002) 385*
[5] Nadiga B.T., An Euler solver based on locally adaptive discrete velocities, *J. Statist. Phys. 81 (1995) 129*
[6] Sun C.H., Adaptive lattice Boltzmann model for compressible flows: viscous and conductive properties, *Phys. Rev. E 61 (4) (2000) 2645*
[7] Chen S.Y., Doolen G.D.,Lattice Boltzmann method for fluid flows, *Annu. Rev. Fluid Mech.,*Vol 30, 1998, pp. 329–364
[8] Lai Y.G., Lin C.L., Huang J., Accuracy and efficiency study of lattice Boltzmann method for steady-state flow simulations, *Numer. Heat Transfer,* B 39, 2001, pp. 21-43
[9] Wolf-Gladrow D.A., Lattice-Gas Cellular Automata and Lattice Boltzmann Models, *Springer, Berlin,* 2000
[10] Clague, D. S., Kandhai, B. D., Zhang, R., Sloot, Hydraulic permeability of (un)bounded fibrous media using the lattice Boltzmann method, *Phys. Rev. E* **61**, 616, P. M. A. (2000)
[11] Kandhai, D., Koponen, A., Hoekstra, A. G., Kataja, M., Timonen, J. & Sloot, Lattice-Boltzmann hydrodynamics on parallel systems. *Comput. Phys. Commun.* **111**, 14, P. M. A. (1998)
[12] Chen S., Martinez D., and Mei R., On boundary conditions in lattice Boltzmann methods, *Physics of Fluids*, 8, 1996, 2527*,* S1070-6631(96)02109-5
[13] Qisu Z. and Xiaoyi H., On pressure and velocity boundary conditions for the lattice Boltzmann BGK model, *Physics of Fluids*, 9(6):1591–1598, June 1997
[14] Koosukuntla N.R., Towards Development of a Multiphase Simulation Model Using Lattice Boltzmann Method (LBM), *Thesis to The University of Toledo,* December 2011
[15] Vanka S. P., Block-implicit multigrid solution of Navier-Stokes equations in primitive variables*, J. Comput. Phys.,* 65, 1986, pp. 138-158
[16] Ghia U., Ghia K. N., Shin C. T., High-Re solutions for incompressible flow using the Navier-Stokes equations and a multigrid method, *J. Comput. Phys.,* 48, 1982, pp. 387-411
[17] Hou S., Zou Q., Chen S., Doolen G., Cogley A., Simulation of Cavity Flow by Lattice Boltzmann Method, 118, 1995, pp. 329-347
[18] Erturk E., Discussions On Driven Cavity Flow, *Int. J. Numer. Meth*, Fluids 60, 2009, pp. 275-294
[19] Chih-Fung H., Cheng C., Kuen-Hau L. and Chao-An L, Consistent Boundary Conditions for 2D and 3D Lattice Boltzmann Simulations, *CMES*, Vol.44, no.2, 2009, pp.137-155
[20] Hazi G., Accuracy of the lattice Boltzmann method based on analytical solutions, *Physical Review E 67, 056705 (2003)*
[21] Moxey D., de Lozar A., Avila M., Barkley D., Hof B., The Onset of Turbulence in Pipe-flow, Science 333, 2011, (6039)192–196.